Early stalked stages in ontogeny of the living isocrinid sea lily *Metacrinus rotundus*

Shonan Amemiya,[1,2,3] Akihito Omori,[4] Toko Tsurugaya,[4] Taku Hibino,[5] Masaaki Yamaguchi,[6] Ritsu Kuraishi,[3] Masato Kiyomoto[2] and Takuya Minokawa[7]

[1]Department of Integrated Biosciences, Graduate School of Frontier Sciences, The University of Tokyo, Kashiwa, Chiba, 277-8526, Japan; [2]Marine and Coastal Research Center, Ochanomizu University, Ko-yatsu, Tateyama, Chiba, 294-0301, Japan; [3]Research and Education Center of Natural Sciences, Keio University, Yokohama, 223-8521, Japan; [4]Misaki Marine Biological Station, Graduate School of Science, The University of Tokyo, Misaki, Kanagawa, 238-0225, Japan; [5]Faculty of Education, Saitama University, 255 Shimo-Okubo, Sakura-ku, Saitama City, 338-8570, Japan; [6]Division of Life Science, Graduate School of Natural Science and Technology, Kanazawa University, Kakuma, Kanazawa, 920-1192, Japan; [7]Research Center for Marine Biology, Tohoku University, Sakamoto 9, Asamushi, Aomori, 039-3501, Japan

Abstract

Amemiya, S., Omori, A., Tsurugaya, T., Hibino, T., Yamaguchi, M., Kuraishi, R., Kiyomoto, M. and Minokawa, T. 2016. Early stalked stages in ontogeny of the living isocrinid sea lily *Metacrinus rotundus*. — *Acta Zoologica* (Stockholm) 97: 102–116.

The early stalked stages of an isocrinid sea lily, *Metacrinus rotundus*, were examined up to the early pentacrinoid stage. Larvae induced to settle on bivalve shells and cultured in the laboratory developed into late cystideans. Three-dimensional (3D) images reconstructed from very early to middle cystideans indicated that 15 radial podia composed of five triplets form synchronously from the crescent-shaped hydrocoel. The orientation of the hydrocoel indicated that the settled postlarvae lean posteriorly. In very early cystideans, the orals, radials, basals and infrabasals, with five plates each in the crown, about five columnals in the stalk, and five terminal stem plates in the attachment disc, had already formed. In mid-cystideans, an anal plate appeared in the crown. Late cystideans cultured in the field developed into pentacrinoids about 5 months after settlement. These pentacrinoids shared many crown structures with adult sea lilies. On the other hand, many features of the stalk differed from those in adult isocrinids, while sharing many characteristics with the stalk of feather star pentacrinoids, including disc-like proximal columnals, high and slender median columnals, synarthrial articulations developmentally derived from the symplexial articulations, limited formation of cirri only in the proximal columnal(s), and an attachment disc. On the basis of these findings, phylogenetic relationships among extant crinoid orders are discussed.

Shonan Amemiya, Marine and Coastal Research Center, Ochanomizu University, Ko-yatsu, Tateyama, Chiba 294-0301, Japan. E-mail: shonan-a@f5.dion.ne.jp

Introduction

Crinoids, comprising the stalked sea lilies and the stalkless comatulids, are widely recognized as a sister group to the other four classes of extant echinoderms and considered to be the most basal of living echinoderms (Paul and Smith 1984; Littlewood *et al.* 1997; Janies 2001; Scouras and Smith 2006; Rouse *et al.* 2013). All extant crinoids belong to the subclass Articulata, which originated from Palaeozoic sea lilies near the start of the Mesozoic era (Ubaghs 1978b; Hess and Ausich 1999; Hess 2011). At present, some of the relationships among the extant orders of articulate crinoids remain controversial (Hess and Messing 2011). For example, although it is now accepted that the comatulids plus the stalked bourgueticrinids are derived within the articulates, there is no consensus about relationships among the more basal stalked orders. One of these basal articulate groups is the order Isocrinida, which includes *Metacrinus rotundus* Carpenter, 1885, the most accessible sea lily known, being relatively abundant at depths of 100–150 m off the southern coast of Japan (Oji 1989). Information on the development of isocrinids is important when considering evolution within the echinoderms in general and the crinoids in particular, and more arguably for discussing evolution of the deuterostomes.

We have previously reported the development of *M. rotundus* between fertilization and larval settlement (Nakano *et al.*

2003). At that time, the swimming larval stages were described in detail, but the settled stages were not characterized substantially because the larvae died soon after they had settled. Here, therefore, we describe the newly settled stages and development throughout the early pentacrinoid stage. This is the first description of these stages based on living material. We focus on the developing skeletal system, to enable comparison with the adult condition and comparable developmental stages of feather stars. The axial organization of the postlarva is discussed based on Carpenter's system of the hydrocoel and surrounding skeletal elements.

Materials and Methods

Animals and larvae

Adults of the isocrinid sea lily *M. rotundus* were collected using a gill net from a depth of 130 m in the south-eastern area of the Uraga Channel in the Sagami Sea, Japan, from late September to middle October. Eggs and sperm were obtained and fertilized, and developmental stages before settlement were cultured as described previously (Amemiya *et al.* 2013). Occasionally, artificial sea water (Jamarin U) containing or lacking antibiotics (100 μg/mL streptomycin and 100 unit/mL penicillin) was used for larval culture. The use of artificial sea water might potentially delay larval development. The antibiotics were effective for keeping the swimming larvae healthy, but reversibly prevented their settlement.

Induction of settlement

To induce settlement of the swimming larvae of *M. rotundus*, we added shell fragments of *Cryptopecten* sp. (a pectinid bivalve collected using a gill net along with the adult sea lilies) to the culture dishes. The larvae became attached to the shells or, less often, to the inner wall of the culture dishes. The settled postlarvae, which initially did not feed, were maintained in a laboratory incubator in the dark at 14 °C. Occasionally, middle to late cystideans were cultured at 16 °C, 18 °C or 20 °C to examine their tolerance to higher temperatures. They grew healthily up to 18 °C, but became weakened and died at 20 °C.

Raising of postlarvae from the late cystidean to pentacrinoid stages

Eleven disposable plastic cups with volumes of 350 mL or 500 mL were used to raise the pentacrinoids. A small fragment of the pectinid shell had been previously glued to the bottom of each cup. The larvae settled on the shells and/or the inner wall of the cups after removal from the culture dishes and developed to the late cystidean stage in the laboratory incubator. At this stage, the cups were glued inside a black bucket, which was then wrapped in a fish net and suspended in the sea at a depth of 3 m from a raft anchored in 8 m of water. The field culture was started on 9 December 2007,

and the settled postlarvae in the cups were examined on 19 March and 3 April 2008.

Preparation of specimens at the early attached stage for scanning electron microscopy (SEM)

Living organisms at the early attached stage were fixed overnight in seawater-Bouin's fluid, dehydrated in a graded ethanol series and critical-point-dried in a CP-5A CO_2 dryer (Topcon, Tokyo, Japan). The dried specimens were attached to aluminium stubs via double-sided adhesive tape, coated with gold in an E-101 ion sputter coater (Hitachi, Tokyo, Japan) and observed with an S-3000N SEM (Hitachi).

Visualization of the skeleton by SEM and polarizing microscopy

Postlarvae at various stages were fixed with 70% ethanol (EtOH) after removal from the substrates. The fixed specimens were rinsed with 70% EtOH and preserved in 70% EtOH at room temperature. The preserved specimens were hydrated with a graded ethanol series, treated with bleach containing 0.4% sodium hypochlorite for 40 s, rinsed with distilled water, dehydrated with a graded ethanol series, air-dried and mounted on an aluminium stub with double-sided electrically conductive adhesive tape. The specimens were occasionally bleached further with the same or a higher (0.6–1.2%) concentration of sodium hypochlorite for the same period or longer (1–2 min) on the adhesive tape stuck to the aluminium stub. The dried specimens were observed with a JSM-6510LV SEM (JEOL, Tokyo, Japan) in back-scattered electron mode to examine the skeletal ossicles. Two very early cystideans were dehydrated with a graded ethanol series after treatment with bleach and photographed in benzyl benzoate and benzyl alcohol (2 : 1) (BABB) under a Biophot (Nikon, Tokyo, Japan) or a BX53F (Olympus, Tokyo, Japan) DIC microscope.

Three-dimensional (3D) reconstruction

A very early cystidean, about 8 days after settlement, and a mid-cystidean, about 19 days after settlement, were fixed with 4% paraformaldehyde for 16 h according to Omori *et al.* (2011). An early cystidean, about 9 days after settlement, was fixed with seawater-Bouin's fluid overnight. After dehydration in a graded ethanol series and transfer through 100% acetone, the specimens were embedded in Technovit 8100 resin (Kulzer, Wehrheim, Germany). Serial 2-μm-thick sections were stained with azure II and methylene blue according to Richardson *et al.* (1960) and photographed under a BX-53F microscope (Olympus). The outer walls of the whole specimen and oral–aboral coelom, inner and outer walls of the postlarval hydrocoel and the outer surfaces of the skeletal chips in each section were traced on the photographs, digitized and reconstructed in 3D using *Reconstruct* software (Fiala 2005).

Results

Induction of larval settlement; early attached stage

In Amemiya *et al.* (2013), we reported that semidoliolaria larvae with incompletely circumferential ciliary bands are competent to settle during the stages from 6 to 12 days postfertilization. At any time during this period, the semidoliolaria larvae would settle on pieces of pecten shells placed in the culture containers. After addition of the shell fragments, the time until settlement varied among the larvae from a few minutes to many hours. Each larva settled when its anterior–ventral end (more specifically, its adhesive concavity) contacted the substrate (Fig. 1A). Attachment appeared to result from conspicuous secretion of coarsely granular material from

the adhesive concavity. Soon after settlement, cilia disappeared from the surface; a few traces of ciliary bands remained, but soon disappeared entirely. The black pigment cells became more uniformly distributed and more crowded in the epidermis (Fig. 1A, inset) as compared with earlier larval stages (Amemiya *et al.* 2013). An open hydropore was detected on the left side of the body, but the position of the closed blastopore was no longer recognizable. The vestibular invagination, now without cilia, appeared to have commenced invaginating to form the vestibular sac.

Living cystideans

A few days after settlement, the early attached stage progressed to the cystidean stage [so named because of its
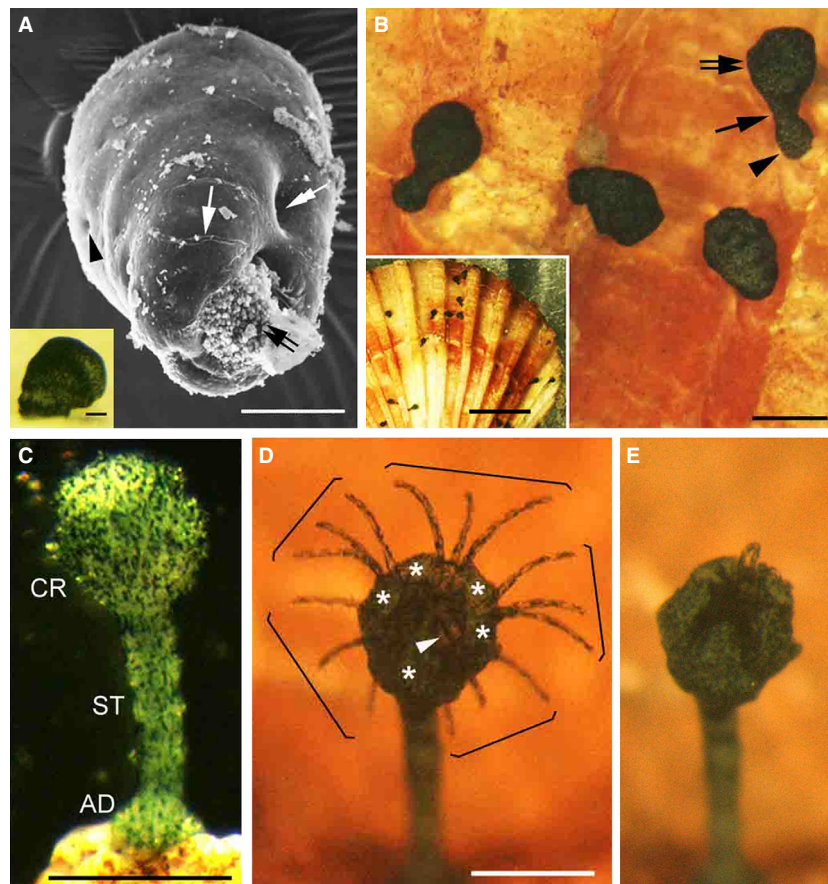
Fig. 1—Development of postlarvae from the early attached to cystidean stages of *M. rotundus*. —**A.** SEM of early attached stage 6.5 days after fertilization (a few hours after settlement), having broken loose from the substrate; left-anterior view. Structures identified include granular material evidently produced by the adhesive concavity (twin arrows); remnants of the ciliary bands (single arrow), vestibular invagination (tandem arrow) and hydropore (arrowhead). Inset: living early attached stage. —**B.** Living early cystideans 24 days after fertilization (~2.5 weeks after settlement), with body comprising crown (twin arrow), stalk (single arrow) and attachment disc (arrowhead) (inset shows same postlarvae at lower power attached to a pecten shell). —**C.** Living mid-cystidean 30 days after fertilization (~2.5 weeks after settlement) with lengthening stalk. —**D.** Living late cystidean 45 days after fertilization (~5.5 weeks after settlement); roof of vestibular sac has been converted into five oral valves (*); triads of radial podia (bracketed) extend through openings that alternate with oral valves; interradial podia (arrowheads). —**E.** Preceding postlarva after withdrawal of radial triads of podia upon mechanical agitation. AD, attachment disc; CR, crown; ST, stalk. Scale line in **A**, **A** inset = 100 μm. Scale line in **B, C, D** (applicable also to **E**) = 500 μm. Scale line in **B** inset = 5 mm.

superficial resemblance to extinct echinoderms of the class Cystoidea (formerly Cystidea)], although the development did not always progress synchronously. The stalk was still short and thick during the early cystidean stage, and the boundary between the stalk and the visceral region (crown) was still indistinct (Fig. 1B). The larvae settled mainly on the concentric troughs of the shells used to induce settlement (Fig. 1B, inset). The settled cystideans leaned to one side, the former ventral side bearing the opening of the vestibular invagination. During development from the early to middle cystidean stage, the stalk became narrower and longer so that the crown and the attachment disc became clearly distinguishable from the stalk (Fig. 1C). As the podia remained hidden by the closed roof of the vestibular sac (Fig. 1B,C), the postlarvae were unable to feed despite continuity of the enteric sac with the vestibular sac (Figs 3A and 4A).

The late cystidean stage (Fig. 1D,E) began about 5.5 weeks after settlement, when the roof of the vestibular sac was converted into five interradial oral valves that opened outward so that the cystideans became capable of feeding. In each radius, the triad of radial podia extended into the openings between the valves (Fig. 1D); mechanical stimulation caused rapid withdrawal of the triad podia as the valves closed (Fig. 1E). In addition, a few interradial podia began growing from the inner surface of each valve.

Internal structures of very early and early cystideans

Tissue sections were prepared from very early cystideans fixed with 4% paraformaldehyde to examine the development of inner organs, especially the skeletal elements and water-vascular system. A section prepared from a very early cystidean at about 8 days after settlement revealed that rotation of the viscera (diagrammed for crinoids generally by Holland 1991) brought the newly formed vestibular sac to the free (now oral) end of the postlarva pointing away from the substrate (Fig. 2A). Skeletal chips were preserved in the section even after cutting with a blade. The floor of the vestibular sac had not yet invaginated so that the mouth and oesophagus had yet to form at this stage. The vestibular sac was underlain by the hydrocoel, which later developed into the water-vascular system. The attached (aboral) end of the cystidean then served as the attachment disc. Three-dimensional (3D) images were reconstructed from 58 serial sections including the one shown in Fig. 2A. The images showed that the hydrocoel is crescent-shaped, comprising five radial lobes (A–E in Carpenter's system), showing the first sign of pentameral symmetry, with a primary stone canal from the C end (Fig. 2B–D). The lumen in the hydrocoel has three evaginations in each lobe. These evaginations are the first indication of the three podia (collectively forming a triad).

In adult crinoids, the mouth and anus form in the central region of the hydrocoel ring (ring canal) and on the CD interray, respectively (de Lussanet 2011). Therefore, the anterior and posterior sides of the postlarva correspond to the sides of

the A radius and CD interradius, respectively (Fig. 2B) (Bather 1900; Ubaghs 1978a). The 3D images of a whole specimen (Fig. 2C,F) indicated that it leans towards the CD interradius, which is the posterior side corresponding to the former ventral side (Fig. 1A,B).

The oral coelom fused with the aboral coelom in some regions to form an oral–aboral coelom (Fig. 2C; Fig. S1, Supporting information). The hydrocoel lies on the surface of the oral–aboral coelom. A total of 20 skeletal plates formed in the calyx (crown), consisting of four layers (circlets) of plates – the orals, radials, basals and infrabasals – each with five plates from top to bottom (Fig. 2D,F,I; Figs S1–S3, Supporting information), indicating that the radial plates had already formed at the very early cystidean stage. The radials and infrabasals formed radially, and the orals and basals interradially, so that the orals and basals alternated with the radials. Five columnals had formed in the stalk (Fig. 2E,F,I; Figs S1 and S2, Supporting information), although the number appeared to vary individually. Each columnal was a fenestrated crescent (Fig. 2G), which would later close to form a ring columnal with a reticulated network (Fig. 5B). In the attachment disc, five terminal stem plates formed (Fig. 2E,H,I; Figs S1 and S4, Supporting information) and appeared to be arranged radially.

A tissue section prepared from an early cystidean fixed with seawater-Bouin's fluid at about 9 days after settlement indicated that the enteric sac establishes a connection with the overlying floor of the vestibular sac through the oesophagus (Fig. 3A), which remained closed at the very early cystidean stage (Fig. 2A). The skeletal ossicles were not preserved in the specimen, because of the acidic fixative. The 3D images indicated that the triad podia in the hydrocoel had developed further and become clearer at this stage (Fig. 3B,C), in comparison with the earlier stage (Fig. 2B–D).

Internal structures of mid-cystideans

A tissue section prepared from a mid-cystidean fixed with 4% paraformaldehyde indicated that the mouth and oesophagus had developed further, and the skeletal chips were clearly preserved (Fig. 4A). 3D images were reconstructed from 90 serial sections including the one shown in Fig. 4A. The triad radial podia in the hydrocoel were well developed (Fig. 4B, C). In addition, some interradial podia had begun to elongate (arrowheads in Fig. 4B inset, C,H). The 3D images indicated that the triad podia formed synchronously in each lobe and that the crescent hydrocoel was not yet closed. The end of the stone canal branched into a hammerhead-like shape (arrow in Fig. 4B). The 3D images of whole specimens (Figs 3C and 4C,E,H) confirmed that the cystideans lean posteriorly. The size of the hydrocoel relative to the oral–aboral coelom increased markedly during development.

In mid-cystideans, the skeleton of the calyx, stalk and attachment disc was composed of reticulated ossicles (Figs 4D–G and 5; Figs S5 and S6, Supporting information). Four layers of calyx plates – the orals, radials, basals and infra-
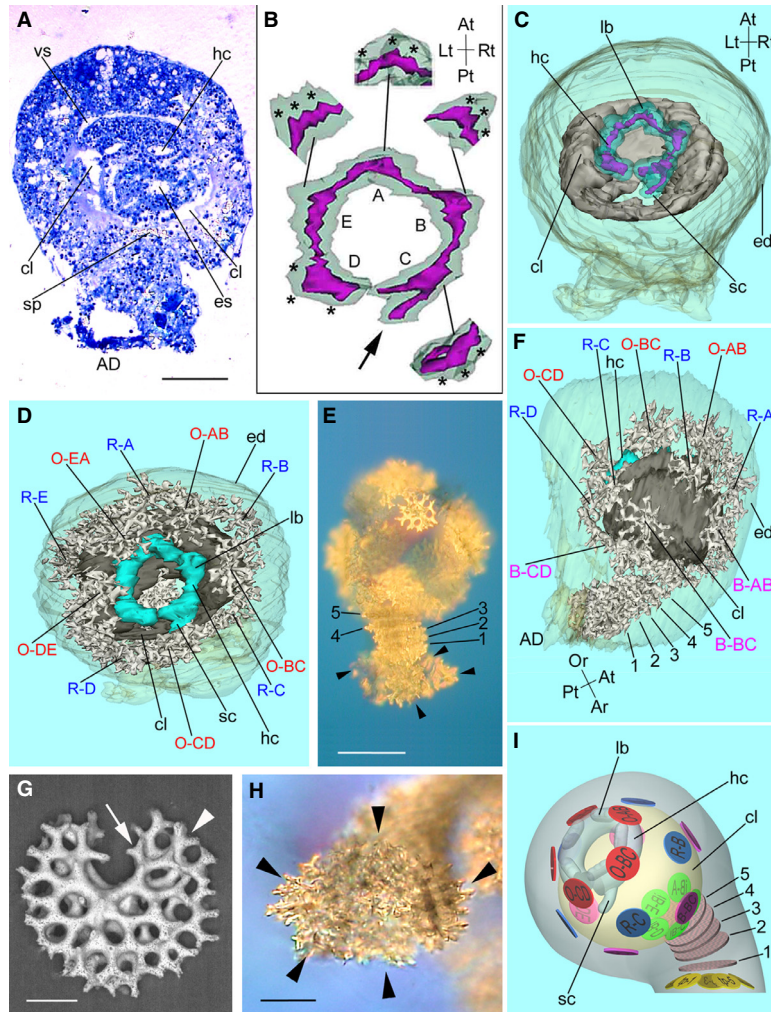
Fig. 2—Very early cystideans of *M. rotundus*. —**A.** Histological section through very early cystidean 17 days after fertilization (~8 days after settlement). —**B.** Hydrocoel of preceding specimen reconstructed from serial sections. 3D image displayed from adoral side, almost perpendicular to plane of hydrocoel. Hydrocoel epidermis half-transparent, showing inner cavity; hydrocoel epidermis (light blue); hydrocoel cavity (purple); hydrocoel lobes designated A–E according to Carpenter's system (insets show lobes A, B, C and E at angles favourable for visualizing the three evaginations from the hydrocoel lumen); evaginations of the hydrocoel lumen (*); primary stone canal (single arrow); orientation of hydrocoel shown at top right according to Ubaghs (1978a). (**C**), (**D**), (**F**) 3D image of whole animal of preceding specimen reconstructed from serial sections; animal epidermises half-transparent, showing internal structures; see Fig. S1 (Supporting information) for movie of 3D-reconstruction including these images. —**C.** Oral (slightly posterior) view; skeletal plates omitted; hydrocoel epidermis half-transparent; orientation of specimen shown at top right. —**D.** Oral view showing arrangement of oral and radial plates (white). —**E.** Polarizing microscopy of another specimen 17 days after fertilization (~8 days after settlement); five columnals (#1–#5) and four (arrowheads) of five terminal stem plates. —**F.** Right-side view showing arrangement of skeletal plates (white) in crown and stalk; columnals numbered 1–5; orientation of specimen shown at bottom. —**G.** SEM of columnals isolated from distal end of stalk in another specimen 15 days after fertilization (~6 days after settlement); two superimposed columnals (arrow and arrowhead). —**H.** Polarizing microscopy of another specimen 17 days after fertilization (~8 days after settlement) showing five terminal stem plates (arrowheads). —**I.** Perspective model of very early cystidean shown in **A–D, F**, viewed from right-posterior with attachment disc at bottom. Skeletal plates comprise four layers – orals (red), radials (blue), basals (pink) and infrabasals (green) – each with five plates in calyx; five columnals (light brown, numbered 1–5) in stalk; five terminal stem plates (yellow) in attachment disc. See Fig. S3 (Supporting information) for movie of perspective 3D model including this image. AD, attachment disc; Ar, aboral; At, anterior; Lt, left; Or, oral; Pt, posterior; Rt, right; cl, oral–aboral coelom; ed, epidermis; es, enteric sac; hc, hydrocoel; lb, lobe; sc, stone canal; sp, spicule; tp, terminal stem plate; vs, vestibule: O-AB, O-BC, O-CD, O-DE and O-EA are orals located in AB, BC, CD, DE and EA interray, respectively. R-A, R-B, R-C, R-D and R-E are radials located in A, B, C, D and E ray, respectively. B-AB, B-BC and B-CD are basals located in AB, BC and CD interray, respectively. iB-A, iB-C, iB-D and iB-E are infrabasals located in A, C, D and E ray, respectively. Scale line in **A, E** = 100 μm. Scale line in **G** = 20 μm. Scale line in **H** = 50 μm.
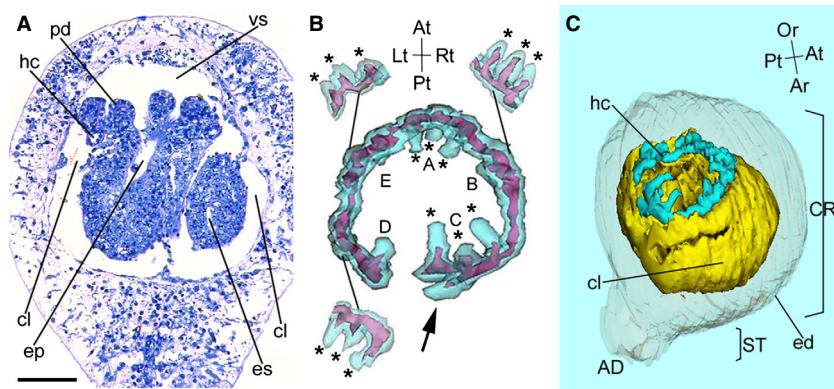
Fig. 3—Early cystidean of *M. rotundus*. —**A.** Histological section through early cystidean 18 days after fertilization (~9 days after settlement). —**B.** Hydrocoel of early cystidean at more advanced stage than Fig. 2B. 3D image reconstructed from 61 serial sections including the one shown in **A**; hydrocoel lobes and primary stone canal indicated as in Fig. 2B; evaginations of hydrocoel lumen developing into podia (*) (insets show lobes B, D and E at angles favourable for visualizing the podia). —**C.** 3D image of whole animal of preceding specimen reconstructed from serial sections; animal epidermis half-transparent; orientation of specimen shown at top right, indicating specimen leans posteriorly. AD, attachment disc; CR, crown; ST, stalk; Ar, aboral; At, anterior; Lt, left; Or, oral; Pt, posterior; Rt, right; cl, oral–aboral coelom; ed, epidermis; ep, oesophagus; es, enteric sac; hc, hydrocoel; pd, podium; vs, vestibule. Scale line in **A** = 50 μm.

basals – each with five plates, were retained at this stage. In addition, an anal plate formed in a region surrounded by four plates, the O-CD, R-C, R-D and B-CD (Fig. 4F,H; Figs S5–S8, Supporting information). Thus, a total of 21 calyx plates had formed at this stage. At the earlier stage, the anal plate was an amorphous spicule (Fig. 4F; Figs S5 and S6A,B, Supporting information), but later it developed into a small circular or elliptical plate (Fig. S8, Supporting information). The infrabasal plates located at the top of the stalk were smaller than the basal plates that alternated with the infrabasals (Fig. 4G). In the stalk, six columnals had formed, and most of them had elongated (Fig. 4E,H) in comparison with the earlier stage (Fig. 2E,F,I).

The stalk was homoeomorphic, that is all the columnals had an essentially similar shape. SEM of partially bleached mid-cystidean revealed six columnals, numbered from the distal (#1) to the proximal (#6) end of the stalk (Fig. 5A). Columnal width was almost constant, but the height varied. Columnals #5 and #6 were thin discs, the latter being particularly thin, whereas the other four columnals were cylindrical. An additional small columnal, designated as #4.5, was revealed between columnals #4 and #5 when the specimen was further bleached (Fig. 5B). The lumen of the axial canal, and the cross sections of the columnals, were circular rather than pentagonal (Fig. 5B, inset). The articular facets of each columnal were symplexies (Fig. 6A) characterized by tooth-like protrusions on both the distal and proximal surfaces.

*Light microscopy of living and fixed pentacrinoids*

The specimens that settled in the 11 plastic cups and were maintained in the laboratory developed to late cystideans at 52 days after fertilization. To raise them further, we then transferred them to the sea. We did not examine the exact number of late cystideans that settled in each of the cups, except for those in two cups that contained, respectively, 21 and 3 individuals. We examined the plastic cups at two time points (152 and 167 days after fertilization) and found a total of ten postlarvae that had survived in three different cups. The first cup contained five postlarvae (Fig. 7A), which were identified as very early pentacrinoids, because each possessed five small arms, a defining feature of this developmental stage (Hyman 1955; Breimer 1978; Holland 1991). Examination of one individual (~7.8 mm in length from an arm tip to the end of the attachment disc) by polarizing microscopy revealed 14 columnals (Fig. 7B), which we numbered from the distal (#1) to the proximal (#14) end. This very early pentacrinoid had a xenomorphic stalk in which apical, median and basal regions were distinguishable from the shape of the columnals. The skeleton of each columnal showed intrinsic birefringence, indicating it was composed of a single crystal of calcite. The second cup contained three other very early pentacrinoids.

The third cup contained two more advanced early pentacrinoids, one larger and one smaller, that had survived for 167 days after fertilization. They were attached close to one another and grew on a shell fragment at the bottom of the cup (Fig. 7C,D). The upper region of the stalk was thicker than the lower region. Both had five arms that were remarkably massive compared to those of feather star pentacrinoids (Mladenov and Chir 1983; Kohtsuka and Nakano 2005). The larger one was about 9.5 mm in length. Each of its arms bore the first and second primibrachs. The second primibrach had two short distal branches (Fig. 7E), the larger one apparently representing the third primibrach, and the smaller one, the first pinnule. Podia projected from the arms. Cirri had formed in the proximal region of the stalk (Fig. 7C–E,G).
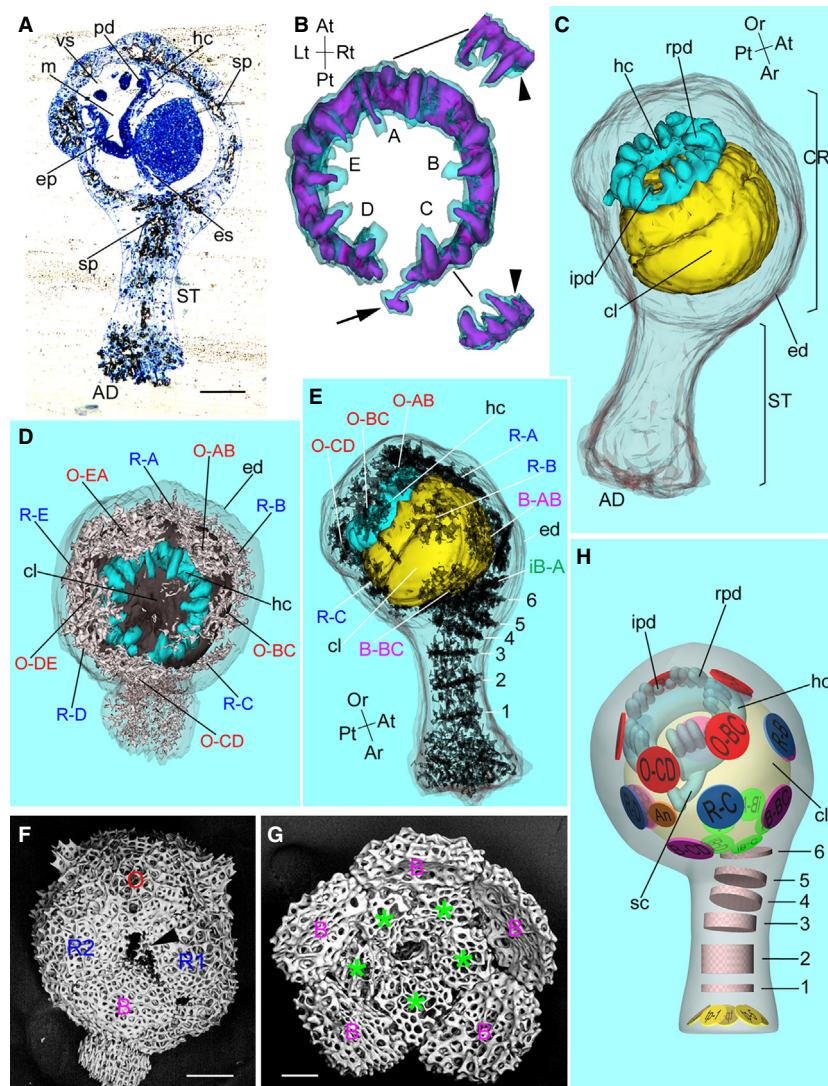
Fig. 4—Mid-cystideans of *M. rotundus*. —**A.** Histological section through mid-cystidean 26 days after fertilization (~19 days after settlement). —**B.** 3D image of hydrocoel of preceding specimen reconstructed from serial sections. Hydrocoel lobes and primary stone canal indicated as in Fig. 2B; insets show lobes A and C at angles favourable for visualizing the interradial podia (arrowheads). (**C, E**) 3D image of whole animal of preceding specimen reconstructed from serial sections; animal epidermises half-transparent; see Fig. S5 (Supporting information) for movie of 3D-reconstruction including these images. —**C.** Right slightly oral view; skeletal plates omitted; orientation of specimen shown at top right. —**D.** Oral view showing arrangement of oral and radial plates (white). —**E.** Right-side view showing arrangement of skeletal plates (black) in crown and stalk; columnals numbered 1–6; orientation of specimen shown at bottom left. (**F, G**) SEM of calyx plates in mid-cystideans at 45 days after fertilization (36 days after settlement) subjected to mild bleaching. —**F.** Whole crown. Amorphous anal plate (arrowhead) is surrounded by four plates designated O, R1, R2 and B in picture, evidently corresponding to O-CD, R-C, R-D and B-CD, respectively. —**G.** Inner surface of lower half of crown cut between radials and basals; five infrabasal plates (*) alternate with five basal plates (B). —**H.** Perspective model of mid-cystidean shown in Fig. 4A–E, viewed from right-posterior with attachment disc at bottom. Skeletal plates comprise four layers – orals (red), radials (blue), basals (pink) and infrabasals (green) – each with five plates, plus anal plate (brown) in calyx; five columnals (light brown, numbered 1–6) in stalk; five terminal stem plates (yellow) in attachment disc. See Fig. S7 (Supporting information) for movie of perspective 3D model including this image. AD, attachment disc; CR, crown; ST, stalk; Ar, aboral; At, anterior; Lt, left; Or, oral; Pt, posterior; Rt, right; cl, oral–aboral coelom; ed, epidermis; ep, oesophagus; es, enteric sac; hc, hydrocoel; ipd, interradial podium; m, mouth; pd, podium; rpd, radial podium; sc, stone canal; sp, spicule; tp, terminal stem plate; vs, vestibule: O-AB, O-BC, O-CD, O-DE, O-EA, R-A, R-B, R-C, R-D, R-E, B-AB, B-BC, iB-A, iB-C, iB-D are same as in Fig. 2. Scale line in **A, F** = 100 μm. Scale line in **G** = 50 μm.
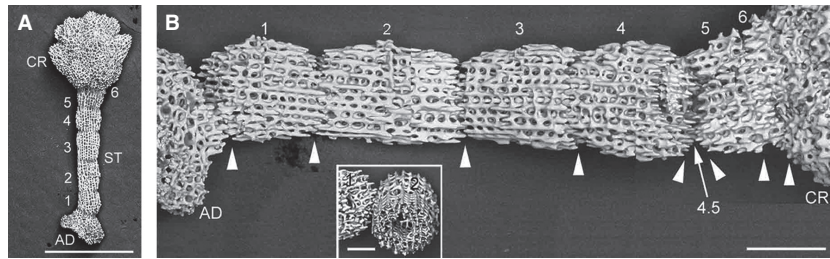
Fig. 5—SEM of skeletal ossicles in *M. rotundus* mid-cystidean. —**A.** Specimen 25 days after fertilization (~2.5 weeks after settlement) subjected to mild bleaching to show skeletal structures. Six columnals, #1, 2, 3, 4, 5 and 6 from distal to proximal, are discernible in the stalk. —**B.** Enlargement of columnal ossicles of **A**, further treated with bleach to show details of articulation and stereom. Intercolumnal ligaments removed almost completely by bleaching. Additional small columnal, #4.5 (arrow); symplexial articulations (arrowheads) (inset shows proximal and distal facets of isolated columnals #1 and #2, respectively). AD, attachment disc; CR, crown; ST, stalk. Scale line in **A** = 500 μm. Scale line in **B** = 100 μm. Scale line in **B** inset = 50 μm.
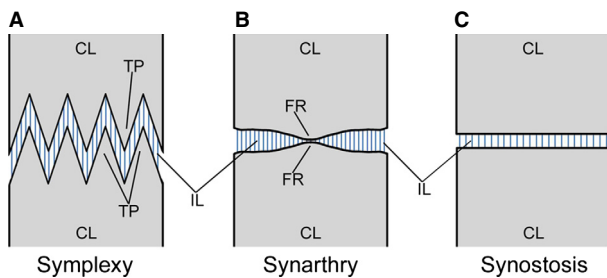
Fig. 6—Schematic drawings of structures of columnal articulations. —**A.** Symplexy; tooth-like protrusions on one facet of a columnal inserted into grooves on opposite facet of another columnal. —**B.** Synarthry; fulcral ridge formed transversely on one facet of a columnal making contact with fulcral ridge on opposite facet of another columnal. —**C.** Synostosis; apposed facets nearly flat. (After Donovan 1984). CL, columnal; FR, fulcral ridge; IL, intercolumnal ligament; TP, tooth-like protrusion.

We fixed the larger of the two more advanced pentacrinoids (except for the distal half of its stalk) in 70% EtOH and examined it under both dissection and polarizing microscopes (Fig. 7F,G, respectively). A mouth occupied the central area of the tegmen, and an anal cone with a terminal anus was located eccentrically, in the posterior part of the tegmen (Fig. 7F). Polarizing microscopy revealed nine columnals (#2–#10) in the upper half of the dissected stalk (Fig. 7G), including five recognizable as nodals (#n1–#n5) and three (#in1–#in3) as internodals. Of the five nodals, #n1 and #n2 were cirrinodals, and #n3, #n4 and #n5 were nudinodals. No cirri were formed in the stalk distal to the #n1 cirrinodal (Fig. 7C,D,G).

SEM of a very early pentacrinoid

The very early pentacrinoid shown in Fig. 7B was slightly bleached to partially remove the soft tissues and allow observation of the skeletal ossicles by SEM. The stalk was separated

by treatment with bleach at the joint between columnals #13 and #14, leaving only #14 attached to the base of the calyx (Fig. 8A,Q). Further treatment with bleach allowed disarticulation of the crown and the apical four columnals into individual ossicles, columnals #11–#14 being isolated as single plates (Fig. 8B,C,I,L–N). Three apical columnals (#12, #13 and #14) were disc-shaped. Columnal #12 was smaller than either #11 or #13. Columnal #11 was longer than those above it, the diameter of its proximal facet being greater than that of its distal facet, which was almost the same as its length. Columnals #2 to #10 were considerably elongated and cylindrical (Figs 7B and 8C–E,H,O,P). Columnals #5, #6 and #7 were particularly long, each almost 0.85 mm in length. The most distal columnal (#1), adjacent to the attachment disc, was quite short (Figs 7B and 8E,F).

Columnals #1 to #10 (Fig. 8C–F,H) all articulated via synarthries (Fig. 6B). The articulation between columnals #10 and #11 (Fig. 8B,C,N) was intermediate between a symplexy (Fig. 6A) and a synarthry. Columnals #11 to #13 (Fig. 8B,C) all articulated via symplexies. The articulation between columnals #13 and #14 (Fig. 8A,L,M) appeared to be a synostosis (Fig. 6C) or symplexy. The articulation between columnal #1 and the stellate attachment disc (Fig. 8E–G) was poorly differentiated. The lumen terminated as a shallow depression in the disc (Fig. 8G).

The stereom of the proximal articular facet of isolated columnal #14 was reticular (Fig. 8I) and consisted of an inner area of small ovoid pores surrounding the central lumen and an outer area with large labyrinthic pores. A narrow groove (black arrowhead in Fig. 8I) separated the two areas, suggesting that a small newly formed columnal with small ovoid pores might fit into the inner area of an older columnal. This possibility was confirmed when a small, wafer-thin ossicle (Fig. 8K) was separated from the larger columnal #14, which bore a shallow depression on its proximal surface, where the small ossicle had been previously lodged (arrow in Fig. 8J). A small, irregular ossicle with many ovoid pores was also found in the inner area on the distal side of columnal #14 (arrow in

Fig. 7—Very early and early pentacrinoids of *M. rotundus*. —**A.** Five very early live pentacrinoids (arrows) settled on inner wall of plastic cup. —**B.** Stalk of very early pentacrinoid. One specimen in **A** fixed with 70% EtOH 152 days after fertilization photographed in BABB by polarizing microscopy. —**C.** Two live early pentacrinoids: larger (large arrow) and smaller (small arrow). —**D.** Same individuals as in **C** viewed from different angle; attachment discs of larger (large arrowhead) and smaller (small arrowhead) specimens. —**E.** Crown and upper region of stalk of larger individual in **C** and **D,** showing arms (arrows), cirri (arrowheads) and podium (tandem arrowhead); lateral view. —**F.** Oral view of specimen in **E,** showing mouth (arrow), anal cone (tandem arrow) and podia (arrowheads). —**G.** Polarizing microscopy of upper region of stalk of specimen in **E** and **F** photographed in BABB; columnals tentatively numbered #2 to #10 from distal to proximal; columnals #3, 5, 7, 9 and 10 corresponding to nodals #n1, n2, n3, n4 and n5, respectively; columnals #4, 6 and 8 corresponding to internodals #in1, in2 and in3, respectively; cirri in cirrinodals #n1 (★) and #n2 (arrowhead). AD, attachment disc; CR, crown; F, first primibrach; P, pinnule; R, radial plate; S, second primibrach; T, third primibrach. Scale line in **A** = 1 cm. Scale line in **B** = 500 μm. Scale line in **C, D** = 2 mm. Scale line in **E** = 1 mm. Scale line in **F** = 400 μm. Scale line in **G** = 200 μm.

Fig. 8L). The proximal surface of columnal #13 was covered with labyrinthic pores in the outer area and with circular pores in the inner area (Fig. 8M). The distal articular facet of columnal #11 had a pair of narrow troughs between a pair of areas with long tooth-like protrusions (arrows in Fig. 8N), indicating the initial transition of the facet from symplexy to synarthry.

Fulcral ridges were clearly identifiable on the facet of the synarthrial articulation in a columnal (#5) when viewed obliquely (arrowheads in Fig. 8O). When a given columnal had synarthrial articulations at both ends, the two fulcral ridges were typically oriented at right angles to one another (Fig. 8C–E,H,O), although in exceptional case, they ran parallel (Fig. 8P). Every columnal was essentially circular in
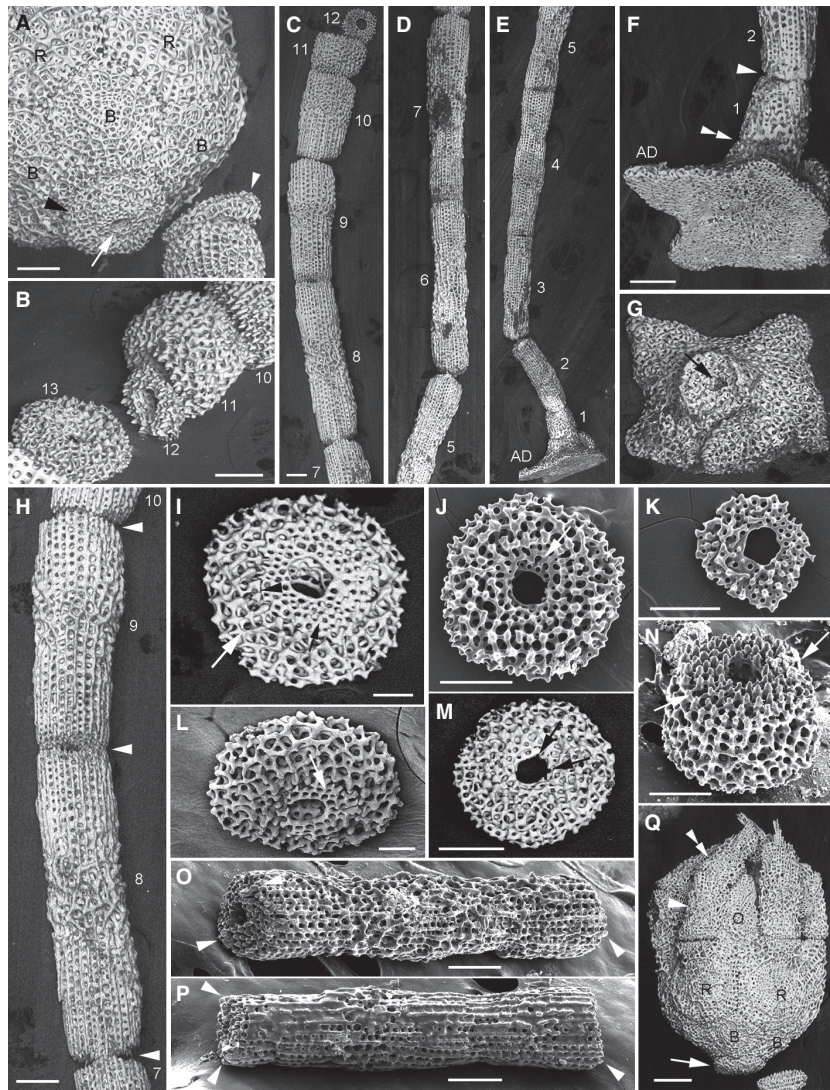
Fig. 8—SEM of skeletal ossicles in very early *M. rotundus* pentacrinoid. —**A.** Basal region of calyx and apical region of stalk in specimen in Fig. 7B. Calyx plates with cog-like protrusions on sutural surfaces engaging as cogwheels; lumen (arrow), and columnals #14 (large black arrowhead) and #13 (small white arrowhead). (**B–H**) Various regions of stalk in specimen in **A**, further treated with bleach. —**B.** Apical region of stalk showing columnals #10–#13. (**C–E**) Most parts of stalk, including columnals #1–#12 and attachment disc. Numbering of columnals corresponds to that in Fig. 7B. —**C.** Upper region of stalk included columnals #8–#12, and proximal half of #7. —**D.** Median region of stalk included columnals #6 and #7, proximal half of #5 and distal end of #8. —**E.** Lower region of stalk included columnals #1–#4, distal half of #5 and attachment disc. —**F.** Enlargement of distal region of stalk; articulations between columnals #1 and #2 (arrowhead) and between columnal #1 and attachment disc (tandem arrowhead). —**G.** Proximal surface of isolated attachment disc with terminus of axial canal (arrow). —**H.** Enlargement of columnals from proximal end of #7 to distal end of #10 with synarthrial articulations (arrowheads); fulcral ridges at proximal and distal ends in columnals #8 and #9 perpendicular to one another. (**I–P**) Isolated single columnals coated with gold after bleaching further observed by SEM under high-vacuum conditions. —**I.** Proximal surface of columnal #14, showing outer (large white arrow) and inner (small black arrow) areas and narrow groove (black arrowhead) bordering both areas. —**J.** Proximal surface of true columnal #14; inner ossicle that occupied inner area in columnal shown in **I** was removed with adhesive tape; shallow depression (arrow) caused by removal of inner ossicle. —**K.** Distal surface of small wafer-thin ossicle removed from inner area of columnal #14. —**L.** Distal-lateral view of columnal #14 with small irregular ossicle (arrow). —**M.** Proximal view of columnal #13 showing marginal irregularities in lumen (arrows). —**N.** Distal-lateral view of columnal #11 showing narrow troughs (arrows) between a pair of areas with long tooth-like protrusions. —**O.** Isolated columnal #5 showing articular facet; fulcral ridges (arrowheads) in proximal and distal ends. —**P.** Isolated columnal #4; fulcral ridges (arrowheads) in proximal and distal ends. —**Q.** Whole view of crown in **A** viewed from different angle; columnal #14 (arrow), and first (arrowhead) and second (tandem arrowhead) primibrachs. AD, attachment disc; B, basal plate; O, oral plate; R, radial plate. Scale line in **A**, **B**, **C** (applicable also to **D** and **E**), **F** (applicable also to **G**), **H**, **J**, **K**, **M**, **N**, **O** and **P** = 100 μm. Scale line in **I** and **L** = 50 μm. Scale line in **Q** = 200 μm.

cross-section, except for a developing small, irregular ossicle nested on the distal facet of columnal #14 (arrow in Fig. 8L). The lumen in every columnal was also essentially circular, except for columnal # 13, which had an ovoid lumen with some marginal irregularities (black arrows in Fig. 8M), and the small ossicle, which had a pentagonal lumen (Fig. 8I,K). The small size of columnal #12 suggested that it is the internodal plate developing between two nudinodals, columnals #11 and #13. Columnal #14 was presumably nudinodal, and the small ossicle (Fig. 8I,K) was a newly developing nudinodal. The small, irregular ossicle (Fig. 8L) was probably the newly developing internodal.

In the whole view of the crown, the developing arms with the first and second primibrachs were clearly discernible (Fig. 8Q). The second primibrachs tapered towards their tips. The radial plates alternated with much smaller basal plates in the calyx (Fig. 8A,Q). The sutures of the calyx plates were symplexies at this stage. The oral plates still remained between the arms.

SEM of an early pentacrinoid

The EtOH-fixed early pentacrinoid that had been dissected in the middle part of the stalk (Fig. 7G) was examined by SEM after slight bleaching. In Fig. 9A, seven columnals are visible – #n1, #in1, #n2, #in2, #n3, #n4 and #n5 – corresponding to columnals #3, #4, #5, #6, #7, #9 and #10 from distal to proximal, respectively, as shown in Fig. 7G. One internodal, #in3, is hidden behind #n3 in this figure. The upper five columnals including #in3 were very thin. Columnals #n2 and #in1 were somewhat elongated, #n1 being cylindrical and considerably longer than the more apical columnals. It appears that the nodals and internodals in pentacrinoids generally formed primarily as thin discs and subsequently elongated into cylinders. Columnals #n4 and #n5 were pentagonal, and #n2 and #n3 were polygonal. The sutures of the calyx plates were synostoses (Fig. 9A,B), as in adults.

The articulations from columnals #1 to #3 were typical synarthries with a fulcral ridge at either end, arranged perpendicular to one another (Fig. 9C,D). These columnals were connected by intercolumnal ligaments on either side of the fulcral ridge in each articulation (Fig. 9C,E). Each end of the ligament penetrated into a galleried pore in the columnal. Grimmer *et al.* (1984) reported that in feather star pentacrinoids, each ligament fibre is composed of numerous parallel collagen fibrils.

The early pentacrinoid had five nodals, two of which (#n1 and #n2) were cirrinodals and three (#n3–#n5) nudinodals (Figs 7G and 9A). Nodal #n1 had comparatively longer triplet cirri, and #n2 had shorter triplet cirri, one of which was remarkably short. The shortest cirrus in #n2 was composed of nine very thin discoidal cirrals (Fig. 9F). Another cirrus on #n2 was slightly more developed (Fig. 9G). Although it consisted of only nine cirrals, as in the shortest cirrus, the first and

second most-proximal cirrals were elongated relative to those in the shortest cirrus. In the #n1 cirrinodal, the most elongated cirrus had 14 cirrals (Fig. 9H). These findings suggest that nine disc-like thin cirrals formed in the primary phase of cirrus formation, followed by elongation from proximal to distal. New cirrals were added after the first nine had become somewhat elongated. The specimen in Fig. 9A was further treated with bleach to remove the cirri from nodal #n1. In Fig. 9I, one cirrus in #n1 has been removed, revealing the cirrus socket, and another has been partially removed, showing the articulation on the most proximal cirral. The surface of the cirrus socket has a nearly circular lumen. The distal articular facet of the most proximal cirral was covered with many tooth-like protrusions. The proximal facet of the second cirral was circular, with tooth-like protrusions (Fig. 9J) and a nearly circular central lumen. In the adult of the isocrinid, *Neocrinus decorus*, the cirral facet was ovoid and the lumen elliptical (Donovan 1984), suggesting that these structures underwent morphological change during development. Both the proximal and distal articulations of the most proximal cirral appeared to be symplexies.

In the crown, the radial and first primibrach articulated via a straight muscular articulation characterized externally by a prominent fulcral ridge (black arrowheads in Fig. 9K). The aboral extensor ligament bundle was lodged in the fossa formed aboral to the fulcral ridge. The interarticular ligament was located adoral to the fulcral ridge (Fig. 9L). Each ligament bundle penetrated into a galleried pore in the stereom, similar to the ligament bundles in the columnal articulations (Fig. 9E).

The five arms surrounded the tegmen (oral view in Fig. 9M). The arms had formed the third and fourth primibrachs, as well as the first three pinnulars in the first pinnule (Fig. 9N). In an image of the same specimen while alive (Fig. 7E), the fourth primibrach was not visible, and the pinnulars were not identifiable in the pinnule because of the lower resolution of the light microscope. Ambulacral and adambulacral plates lined the oral side of the brachials and pinnulars (Fig. 9O).

Discussion

Survival potential of M. rotundus *postlarvae at shallow sea depth*

In this study, we succeeded in raising settled postlarvae of the sea lily *M. rotundus* through the early pentacrinoid stage by rearing them in the sea near the surface. During field culture, the temperature of the sea water varied within the range 10.5–17.5 °C. *M. rotundus* adults typically live at a depth of about 130 m, where the annual change in water temperature is estimated to be within the range 12–16 °C. The results of our experiment showed that the late cystideans and pentacrinoids of *M. rotundus* have the potential to survive and grow under conditions near the sea surface as long as the temperature does not greatly vary from the range at 130 m.
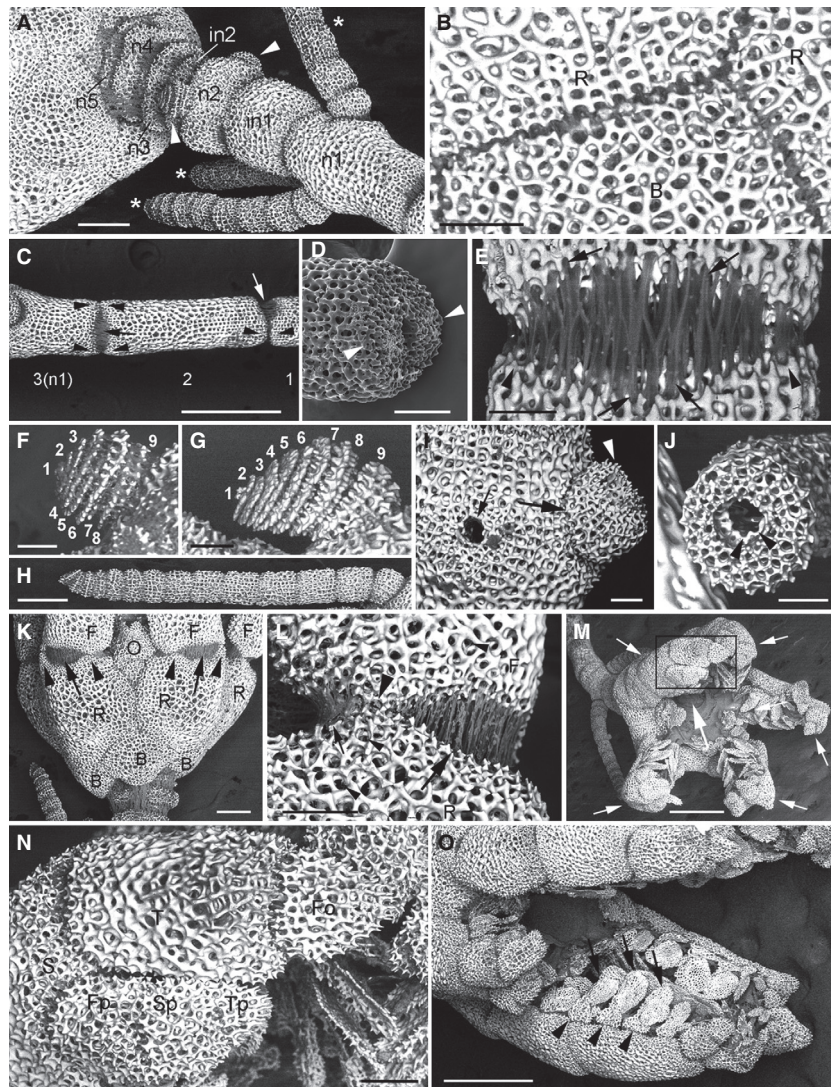
Fig. 9—SEM of skeletal ossicles in early *M. rotundus* pentacrinoid. —**A.** Basal region of calyx and apical region of stalk in specimen in Fig. 7E–G; 3 (*) of 3 and 2 (arrowheads) of 3 cirri on cirrinodals #n1 and #n2, respectively. —**B.** Sutural contacts in calyx plates. —**C.** Columnals #1–#3, showing typical synarthrial articulations with ligaments (arrows) and fulcral ridges (arrowheads). —**D.** Enlargement of fulcral ridge (arrowheads) at a facet of synarthrial articulation in columnal #2 isolated from specimen in **C.** —**E.** Enlargement of intercolumnal ligaments (arrows) and fulcral ridge (arrowheads) at synarthrial articulation of 2 adjacent columnals. —**F.** Early-stage cirrus in nodal #n2; cirral ossicles in cirrus numbered from #1 to #9 from tip to base. —**G.** Slightly more advanced cirrus in nodal #n2; cirral ossicles indicated by **F.** —**H.** Most elongated cirrus in nodal #n1. —**I.** Nodal #n1 with one cirrus removed completely, and another removed mostly leaving only the most proximal cirral; lumen (small arrow), most proximal cirral (large arrow) and tooth-like protrusions (arrowhead). —**J.** Proximal articular facet of second proximal cirral; marginal irregularities in lumen (arrowheads). —**K.** Calyx and first primibrachs of arms; aboral extensor ligament bundles (arrows) and both ends of two fulcral ridges (arrowheads). —**L.** Enlargement of articulation between radial plate and first primibrach; aboral extensor ligaments (large arrow), interarticular ligaments (small arrow), fulcral ridge (large arrowhead) and galleried pores (small arrowheads). —**M.** Oral view of crown; oral area (large arrow) and arms (small arrows). —**N.** Enlargement of rectangle in **M**, showing primibrachs and pinnulars in an arm. —**O.** Enlargement of arms; ambulacral (arrows) and adambulacral plates (arrowheads). B, basal plate; F, first primibrach; Fo, fourth primibrach; Fp, first pinnular; O, oral plate; R, radial plate; S, second primibrach; Sp, second pinnular; T, third primibrach; Tp, third pinnular. Scale line in **A, H** and **K** = 200 μm. Scale line in **B, D, L** and **N** = 100 μm. Scale line in **C, M** and **O** = 500 μm. Scale line in **E, F, G, I** and **J** = 50 μm.

The calyx in the M. rotundus *postlarva*

The postlarvae of *M. rotundus* began to form the five radial groups of triad podia after settlement (Figs 2A–D,I, 3A–C and 4A–D,H). In the feather star species *Tropiometra carinata*, *Compsometra* (*Antedon*) *serrata* (Mortensen 1920) and *Antedon adriatica* (*mediterranea*) (Bury 1888), the larvae develop podia

as early as the late doliolaria stage. Thus, in feather star larvae, the podia begin to form earlier. During feather star development, the dipleurula stage is omitted, and the uniformly ciliated larva develops into a doliolaria larva almost directly (Holland 1991). This abbreviated development of feather stars can be correlated with the shift in timing of podia formation to earlier stages.

When the oral valves opened, a total of 15 podia extended from the opening in the cystidean of *M. rotundus* (Fig. 1D). These 15 podia consisted of five radial groups of triad podia. Similar to the situation in *M. rotundus*, 15 radial podia, each composed of five triplets, ultimately extend from the oral opening in feather star cystideans (Hyman 1955), and two different modes for the final completion of these podia have been reported. In one case, described for *A. adriatica* (Bury 1888; Seeliger 1892) and *T. carinata* (Mortensen 1920), five knob-like evaginations appear radially on the crescent hydrocoel, followed by development of three branches from the distal end of each, thus forming five groups of triad podia. In the other case, reported for *Oxycomanthus japonicus* (Dan 1968) and *Decametra tigrina* (Kohtsuka and Nakano 2005), five pairs of radial podia are formed first, then a podium is added peripherally on the radii to each pair, and eventually, 15 podia are completed. 3D image analysis of *M. rotundus* postlarvae showed that five lobes are first formed in the crescent hydrocoel. The triad podia are then formed synchronously in each lobe. This process has some similarity with the first case for *A. adriatica* and *T. carinata* and is distinct from the second case reported for *O. japonicus* and *D. tigrina*, suggesting that the first case is the ancestral mode.

In feather stars, the oral and aboral coeloms are derived from the left and right somatocoels, respectively, formed at the doliolaria stage (Hyman 1955; Breimer 1978). Our study indicated that the oral coelom fuses with the aboral coelom in some regions, making it difficult to distinguish them as different coeloms (Figs 2C, 3C and 4C; Figs S1 and S5, Supporting information). Therefore, we considered these coeloms to be one continuous coelom and designated it as an oral–aboral coelom. Our preliminary observations indicated that the left somatocoel fuses with the right somatocoel at the semidoliolaria stage.

In feather stars, five radial plates typically appear just before arm elongation, and the appearance of the plates is considered to be the first sign of a crinoid's arrival at the pentacrinoid stage (Breimer 1978). The timing of radial plate formation is remarkably advanced in *M. rotundus*, the radial plates being evident in the very early cystidean and comparable in size to the orals and basals (Fig. 2D,F,I; Figs S1 and S2, Supporting information). Although the reason for this advanced timing in *M. rotundus* is still unclear, we assume that the visceral mass volume in early-stage *M. rotundus* postlarvae might be larger than that of feather stars so that the postlarvae need more calyx plates. Based on the late appearance of the radials in feather stars, it has been proposed that

the radials are not true calyx plates, but the first plates of the brachial series (Hyman 1955). Our results suggest that the radials are true calyx plates for protecting the visceral mass in the postlarvae and that the function of the plates is inherited from the common ancestor of the crinoids. Most fossil crinoids have a well-developed calyx (Ubaghs 1978a), supporting this function.

In feather stars, the anal plate forms just before or soon after the appearance of the radial plates (Breimer 1978). In the mid-cystideans of *M. rotundus*, the anal plate appeared considerably earlier than it does in feather stars, probably as a result of the advanced formation of the radial plates. The calyx plates are regularly arranged at the very early cystidean stage (Fig. 2D,F; Figs S1 and S2, Supporting information). The size and location of the plates neighbouring the anal plate, that is the C and D radials and the CD interradial basal, are remarkably disturbed at the mid-cystidean stage (Fig. 4F; Figs S5 and S6A,B, Supporting information), evidently because of the later insertion of the anal plate. Similar disarrangement of the posterior plates has been reported for some Palaeozoic crinoids (Ubaghs 1978a). The anal plate(s) has been reported for Palaeozoic crinoids and living feather stars, but not for extant stalked crinoids (Hyman 1955; Breimer 1978; Ubaghs 1978a; T. Oji, personal communication). Our finding represents the first record of the anal plate in recent stalked crinoids.

The stalk in the *M. rotundus postlarva*

The upper columnals in the stalk of the *M. rotundus* mid-cystidean were very thin, indicating that the new columnal was formed at the boundary of the basal extremity of the calyx and the proximal end of the stalk, as reported for feather stars (Thomson 1865; Lahaye and Jangoux 1987). However, we found that another small ossicle was hidden between two columnals (Fig. 5B), indicating that in *M. rotundus* cystideans, a new columnal is formed not only at the basal extremity of the calyx but also between the columnals. The columnal plates, being thin fenestrated crescents at the very early cystidean stage (Fig. 2G), developed into reticulated cylinders or discs (Fig. 5B), similar to those of feather stars (Bury 1888; Mortensen 1920).

The mid-cystidean of *M. rotundus* had a homoeomorphic stalk with seven columnals in which the articulations were all symplexies (Fig. 5B). The very early pentacrinoid that we raised had a xenomorphic stalk with 14 columnals, of which the distal 11 had synarthrial articulations (Fig. 8). These results indicated that the articulation structures change from symplexies to synarthries during development of the postlarva from the cystidean to the pentacrinoid stage. Similar changes have been reported for the articulations in feather star columnals (Lahaye and Jangoux 1987; Shibata *et al.* 2008). Synarthrial articulations in young isocrinids have been reported by Clark (1908) for the extant *N. decorus* and by Jaeger

(1985) for the extinct *Balanocrinus subsulcatus* (=*B. subteroides*).

Gislén (1924) reported that in young specimens of an isocrinid, *Metacrinus* sp., some of the most distal columnals lack cirri and that the cirrus whorl is not pentamerous. The early pentacrinoid we studied had two cirrinodals, #n1 and #n2, both bearing triplet cirri (Figs 7E,G and 9A). Moreover, no cirri were formed in the stalk distal to the #n1 cirrinodal, indicating that the non-pentamerous arrangement of cirri originates at the earliest pentacrinoid stage of isocrinids.

In feather stars, the attachment disc is composed of a single terminal stem plate (Hyman 1955), whereas in *M. rotundus* it consists of five terminal stem plates (Figs 2H,I and 4H; Figs S1, S4 and S5, Supporting information). Therefore, the single terminal stem plate may have evolved from the multiple-plate ancestral condition.

The early pentacrinoids that we raised in this study have many structures in the crown that are characteristic of adult sea lilies, such as radial plates, straight muscular articulations, primibrachs, pinnules, cover plates, a mouth and an anal cone. In the stalk, *M. rotundus* pentacrinoids had a considerable number of features that differed from those of adults. The adult isocrinid sea lilies, which include *M. rotundus*, have a heteromorphic stalk composed of nodal and internodal columnals that are low, pentagonal or circular, with a central lumen (Donovan 1984; Oji 1989). Each columnal is markedly broader than its height. Most articulations in the columnals are symplexies, except for some synostosial articulations (Macurda and Meyer 1975; Donovan 1984; Ausich *et al.* 1999). Each nodal bears a circlet of five cirri. Adult isocrinid sea lilies do not have an attachment disc that functions as a holdfast for attachment to a solid substrate (Rasmussen and Sieverts-Doreck 1978). Instead, the adults grasp the substrate using their cirri (Breimer 1978). In contrast to adults, the pentacrinoids of *M. rotundus* adhered to the substrate by the attachment disc.

The pentacrinoid stalk of *M. rotundus* and that of feather stars share many characteristics including disc-like proximal columnals, high and slender mid-stalk columnals, synarthrial articulations developmentally derived from the symplexies in the middle and distal columnals, formation of cirri limited to the proximal columnal(s), and an attachment disc. These similarities suggest two possible phylogenetic relationships among the orders of extant crinoids: either isocrinids and feather stars are closely related, as proposed by many researchers (Rasmussen 1978; Simms 1988; Heinzeller 1998; Hess 2011), or these common characteristics are more ancestral within the subclass Articulata and have persisted in relatively distantly related isocrinid and feather star lineages. A recent molecular phylogenetic study has suggested that isocrinids are the most basal group of extant articulates (Rouse *et al.* 2013), supporting the second possibility. To clarify which of these possibilities is more likely, it would be helpful to record the ontogeny of some other lineages of stalked crinoids, especially cyrtocrinids and hyocrinids. Further phylogenetic analyses, both morphological and molecular, based on as many data as possible over a wide spectrum of taxa, would also be important.

Acknowledgements

Supporting Information

Additional supporting information may be found in the online version of this article:

Fig. S1 Movie of 3D-reconstruction of very early cystidean shown in Fig. 2A–D,F; animal epidermis half-transparent.

Fig. S2 Static images prepared from movie of 3D-reconstruction shown in Fig. S1 (Supporting information), indicating skeletal elements (white); animal epidermis omitted; all 20 calyx plates consisting of five orals, five radials, five basals and five infrabasals shown in A or B.

Fig. S3 Movie of perspective 3D model of very early cystidean shown in Fig. S1 (Supporting information).

Fig. S4 SEM of 5 terminal stem plates isolated from mid-cystidean (A), and attachment disc with 5 terminal stem plates in late cystidean (B) subjected to bleaching.

Fig. S5 Movie of 3D-reconstruction of mid-cystidean shown in Fig. 4A–E.

Fig. S6 Static images prepared from movie of 3D-reconstruction shown in Fig. S5 (Supporting information), indicating skeletal elements (black); animal epidermises omitted; all 21 calyx plates consisting of five orals, five radials, five basals, five infrabasals and an anal plate shown in A, B or C.

Fig. S7 Movie of perspective 3D model of mid-cystidean shown in Fig. S5 (Supporting information).

Fig. S8 SEM of skeletal ossicles in calyx of late cystidean subjected to mild bleaching, showing anal plate (★).

References

Amemiya, S., Hibino, T., Nakano, H., Yamaguchi, M., Kuraishi, R. and Kiyomoto, M. 2013. Development of ciliary bands in larvae of the living isocrinid sea lily *Metacrinus rotundus*. *Acta Zoologica*. doi: 10.1111/azo.12049.

Ausich, W. I., Brett, C. E., Hess, H. and Simms, M. J. 1999. Crinoid form and function. In: Hess, H., Ausich, W. I., Brett, C. E. and Simms, M. J. (Eds): Fossil Crinoids, pp. 3–30. Cambridge University Press, Cambridge, UK.

Bather, F. A. 1900. The Echinodermata. The Pelmatozoa. In: Lankester, E. R. (Ed.): A Treatise on Zoology, Pt. 3, The Crinoidea, pp. 94–204. Adam and Charles Black, London, UK.

Breimer, A. 1978. General morphology—Recent crinoids. In: Moore, R. C. and Teichert, C. (Eds): Treatise on Invertebrate Paleontology, Part T, Echinodermata 2, Vol. 1, pp. 9–58. The University of Kansas, Lawrence, KS.

Bury, H. 1888. The early stages in the development of *Antedon rosacea*. *Philosophical Transactions of the Royal Society of London B* **179**: 257–301 + plates 43–47.

Clark, A. H. 1908. The axial canals of the recent *Pentacrinitidae*. *Proceedings of the United States National Museum* **35**: 87–91.

Dan, K. 1968. Echinoderma. In: Kume, M. and Dan, K. (Eds): Invertebrate Embryology, pp. 280–315 + 329–331. Prosveta Press, Belgrade, Yugoslavia.

Donovan, S. K. 1984. Stem morphology of the recent crinoid *Chladocrinus* (*Neocrinus*) *decorus*. *Palaeontology* **27**: 825–841.

Fiala, J. C. 2005. Reconstruct: A free editor for serial section microscopy. *Journal of Microscopy* **218**: 52–61.

Gislén, T. 1924. Echinoderm studies. *Zoologiska Bidrag Fran Uppsala* **9**: 1–316.

Grimmer, J. C., Holland, N. D. and Kubota, H. 1984. The fine structure of the stalk of the pentacrinoid larva of a feather star, *Comanthus japonica* (Echinodermata: Crinoidea). *Acta Zoologica* **65**: 41–58.

Heinzeller, T. 1998. The nervous system of crinoids: survey and taxonomic implications. In: Mooi, R. and Telford, M. (Eds): Echinoderms: San Francisco, pp. 169–174. A. A. Balkema, Rotterdam.

Hess, H. 2011. Articulata: introduction. In: Selden, P. A. (Ed.): Treatise on Invertebrate Paleontology, Part T, Echinodermata 2, Revised, Crinoidea, Vol. 3, pp. 1–22. The University of Kansas, Lawrence, KS.

Hess, H. and Ausich, W. I. 1999. Introduction. In: Hess, H., Ausich, W. I., Brett, C. E. and Simms, M. J. (Eds): Fossil Crinoids, pp. xiii–xv. Cambridge University Press, Cambridge, UK.

Hess, H. and Messing, C. G. 2011. Comatulida. In: Selden, P. A. (Ed.): Treatise on Invertebrate Paleontology, Part T, Echinodermata 2, Revised, Crinoidea, Vol. 3, pp. 70–159. The University of Kansas, Lawrence, KS.

Holland, N. D. 1991. Echinodermata: Crinoidea. In: Giese, A. C., Pearse, J. S. and Pearse, V. B. (Eds): Reproduction of Marine Invertebrates, Echinoderms and Lophophorates, Vol. 4, pp. 247–299. Boxwood Press, Pacific Grove, CA.

Hyman, L. H. 1955. The Invertebrates. Echinodermata: The Coelomate Bilateria, Vol. 4. McGraw-Hill Book Company, New York.

Jaeger, M. 1985. Die Crinoiden aus dem Pliensbachium (mittlerer Lias) von Rottorf am Klei und Empelde (Sud-Niedersachsen). *Bericht der Naturhistorischen Gesellschaft zu Hannover* **128**: 71–151.

Janies, D. 2001. Phylogenetic relationships of extant echinoderm classes. *Canadian Journal of Zoology* **79**: 1232–1250.

Kohtsuka, H. and Nakano, H. 2005. Development and growth of the feather star *Decametra tigrina* (Crinoidea), with emphasis on the morphological differences between adults and juveniles. *Journal of the Marine Biological Association of the United Kingdom* **85**: 1503–1510.

Lahaye, M. C. and Jangoux, M. 1987. The skeleton of the stalked stages of the comatulid crinoid *Antedon bifida* (Echinodermata). *Zoomorphology* **107**: 58–65.

Littlewood, D. T. J., Smith, A. B., Clough, K. A. and Emson, R. H. 1997. The interrelationships of the echinoderm classes: Morphological and molecular evidence. *Biological Journal of the Linnean Society* **61**: 409–438.

de Lussanet, M. H. E. 2011. A hexamer origin of the echinoderms' five rays. *Evolution & Development* **13**: 228–238.

Macurda, D. B. and Meyer, D. L. 1975. The microstructure of the crinoid endoskeleton. In: Teichert, C. (Ed.): The University of Kansas Paleontological Contributions, Paper 74, pp. 1–22 + plates 1–30. The University of Kansas, Lawrence, KS.

Mladenov, P. V. and Chir, F. S. 1983. Development, settling behaviour, metamorphosis and pentacrinoid feeding and growth of the feather star *Florometra serratissima*. *Marine Biology* **73**: 309–323.

Mortensen, T. 1920. Studies in the development of crinoids. *Papers from the Department of Marine Biology* 16: i–v + I–94 + I-plates XXVIII. Carnegie Institution of Washington, Washington.

Nakano, H., Hibino, T., Oji, T., Hara, Y. and Amemiya, S. 2003. Larval stages of a living sea lily (stalked crinoid echinoderm). *Nature* **421**: 158–160.

Oji, T. 1989. Growth rate of stalk of *Metacrinus rotundus* (Echinodermata: Crinoidea) and its functional significance. *Journal of the Faculty of Science, University of Tokyo, Section 2* **22**: 39–51.

Omori, A., Akasaka, K., Kurokawa, D. and Amemiya, S. 2011. Gene expression analysis of *Six3*, *Pax6*, and *Otx* in the early development of the stalked crinoid, *Metacrinus rotundus*. *Gene Expression Patterns* **11**: 48–56.

Paul, C. R. C. and Smith, A. B. 1984. The early radiation and phylogeny of echinoderms. *Biological Reviews* **59**: 443–481.

Rasmussen, H. W. 1978. Evolution of articulate crinoids. In: Moore, R. C. and Teichert, C. (Eds): Treatise on Invertebrate Paleontology, Part T, Echinodermata 2, Vol. 1, pp. 302–316. The University of Kansas, Lawrence, KS.

Rasmussen, H. W. and Sieverts-Doreck, H. 1978. Classification. In: Moore, R. C. and Teichert, C. (Eds): Treatise on Invertebrate Paleontology, Part T, Echinodermata 2, Vol. 1, pp. 813–928. The University of Kansas, Lawrence, KS.

Richardson, K. C., Jarrett, L. and Finke, E. H. 1960. Embedding in epoxy resin for ultrathin sectioning in electron microscopy. *Stain Technology* **35**: 313–323.

Rouse, G. W., Jermiin, L. S., Wilson, N. G., Eeckhaut, I., Lanterbecq, D., Oji, T., *et al.* 2013. Fixed, free and fixed: The fickle phylogeny of extant Crinoidea (Echinodermata) and their Permian-Triassic origin. *Molecular Phylogenetics and Evolution* **66**: 161–181.

Scouras, A. and Smith, M. J. 2006. The complete mitochondrial genomes of the sea lily *Gymnocrinus richeri* and the feather star *Phanogenia gracilis*: Signature nucleotide bias and unique nad4L gene rearrangement within crinoids. *Molecular Phylogenetics and Evolution* **39**: 323–334.

Seeliger, O. 1892. Studien zur Entwicklungsgeschichte der Crinoiden (*Antedon rosacea*). *Zoologische Jahrbücher Abteilung für Anatomie und Ontogenie der Tiere* **6**: 161–444.

Shibata, T. F., Sato, A., Oji, T. and Akasaka, K. 2008. Development and growth of the feather star *Oxycomanthus japonicus* to sexual maturity. *Zoological Science* **25**: 1075–1083.

Simms, M. J. 1988. The phylogeny of post-Palaeozoic crinoids. In: Paul, C. R. C. and Smith, A. B. (Eds): Echinoderm Phylogeny and Evolutionary Biology, pp. 269–284. Clarendon Press, Oxford.

Thomson, W. 1865. On the embryogeny of *Antedon rosaceus*, Linck (*Comatula rosacea* of Lamarck). *Philosophical Transactions of the Royal Society of London* **155**: 513–544.

Ubaghs, G. 1978a. Skeletal morphology of fossil crinoids. In: Moore, R. C. and Teichert, C. (Eds): Treatise on Invertebrate Paleontology, Part T, Echinodermata 2, Vol. 1, pp. 58–216. The University of Kansas, Lawrence, KS.

Ubaghs, G. 1978b. Origin of crinoids. In: Moore, R. C. and Teichert, C. (Eds): Treatise on Invertebrate Paleontology, Part T, Echinodermata 2, Vol. 1, pp. 275–281. The University of Kansas, Lawrence, KS.